RESEARCH ARTICLE

Online Mapping With the Deep Brain Stimulation Lead: A Novel Targeting Tool in Parkinson's Disease

Luka Milosevic, PhD,[1] Maximilian Scherer, MSc,[1] Idil Cebi, MD,[1,2] Robert Guggenberger, PhD,[1] Kathrin Machetanz, MD,[1] Georgios Naros, MD,[1] Daniel Weiss, MD,[2] and Alireza Gharabaghi, MD[1*]

[1]*Division of Functional and Restorative Neurosurgery, Department of Neurosurgery, and Tübingen NeuroCampus, University of Tübingen, Tübingen, Germany*
[2]*Centre for Neurology, Department for Neurodegenerative Diseases, and Hertie Institute for Clinical Brain Research, University Tübingen, Tübingen, Germany*

ABSTRACT: Background: Beta-frequency oscillations (13–30 Hz) are a subthalamic hallmark in patients with Parkinson's disease, and there is increased interest in their utility as an intraoperative marker.
Objectives: The objectives of this study were to assess whether beta activity measured directly from macrocontacts of deep brain stimulation leads could be used (a) as an intraoperative electrophysiological approach for guiding lead placements and (b) for physiologically informed stimulation delivery.
Methods: Every millimeter along the surgical trajectory, local field-potential data were collected from each macrocontact, and power spectral densities were calculated and visualized (n = 39 patients). This was done for online intraoperative functional mapping and post hoc statistical analyses using 2 methods: generating distributions of spectral activity along surgical trajectories and direct delineation (presence versus lack) of beta peaks. In a subset of patients, this approach was corroborated by microelectrode recordings. Furthermore, the match rate between beta peaks at the final target position and the clinically determined best stimulation site were assessed.
Results: Subthalamic recording sites were delineated by both methods of reconstructing functional topographies of spectral activity along surgical trajectories at the group level ($P < 0.0001$). Beta peaks were detected when any portion of the 1.5 mm macrocontact was within the microelectrode-defined subthalamic border. The highest beta peak at the final implantation site corresponded to the site of active stimulation in 73.3% of hemispheres ($P < 0.0001$). In 93.3% of hemispheres, active stimulation corresponded to the first-highest or second-highest beta peak.
Conclusions: Online measures of beta activity with the deep brain stimulation macroelectrode can be used to inform surgical lead placement and contribute to optimization of stimulation programming procedures.

Key Words: beta oscillations; deep brain stimulation; Parkinson's disease; subthalamic nucleus

Deep brain stimulation (DBS) of the subthalamic nucleus (STN) is a well-established and efficacious therapy for the management of the motor symptoms of Parkinson's disease.[1,2] Many factors contribute to the clinical benefit of STN-DBS, including patient selection, stimulation programming, medication adjustments, and disease progression.[3,4] However, one important factor that may preclude other clinically controllable factors is the proper placement of the DBS lead.[5-7] A study that assessed lead placements in more than 28,000 cases (from 2 large North American databases) identified staggeringly high rates of revision and removal, between 15.2% and 34.0%, with up to 48.5% being attributed to improper targeting or lack of therapeutic efficacy.[8] In another study that investigated 41 consecutive patients who complained about suboptimal results from their DBS devices, 46% were identified as having misplaced leads.[9] Misplaced leads not only limit therapeutic efficacy but also can give

*Correspondence to: Dr. Alireza Gharabaghi, Division of Functional and Restorative Neurosurgery, Eberhard Karls University Tuebingen, Otfried-Mueller-Str.45, 72076 Tuebingen, Germany; E-mail: alireza.gharabaghi@uni-tuebingen.de

Relevant conflicts of interests/financial disclosures: Nothing to report.

Funding agency: This work was supported by grants from the University of Tübingen and Abbott.

Received: 12 December 2019; **Revised:** 16 April 2020; **Accepted:** 17 April 2020

Published online 18 May 2020 in Wiley Online Library (wileyonlinelibrary.com). DOI: 10.1002/mds.28093

rise to intolerable motor and/or nonmotor side effects.[10,11] As such, maximized efforts toward proper lead positioning prior to and during STN-DBS surgeries are warranted.

The traditional approach for determining the implantation site of the DBS macroelectrode is a multistep process. The position is tentatively determined based on a fusion of preoperative magnetic resonance imaging (MRI) and computed tomography images used in conjunction with stereotactic atlases to determine the stereotactic coordinates of the tentative target location.[12] The radiologically defined anatomical target is then corroborated by an intraoperative electrophysiological mapping procedure in combination with test stimulation prior to the final DBS macroelectrode implantation. Microelectrode recording (MER) of single unit activity is the gold-standard electrophysiological approach used for identification of the implantation target. This procedure involves delineation of anatomical structures along the surgical trajectory based on characteristic neuronal firing properties,[13] propensity for oscillatory behavior in the spike train,[14] and responsiveness to active or passive movements of the contralateral limbs.[15]

Although electrophysiological confirmation of the target location is considered a crucial and arguably necessary step,[5,16] some centers choose to forego MER mapping procedures in favor of reducing surgical time and increasing tolerance, due to a lack of dedicated personnel or resources, and/or the risk of hemorrhage. Image-guided-only surgeries have the additional benefit of being able to be performed while the patient is under general anesthesia, whereas in electrophysiology-driven approaches the patient is most often awake. The consequence of foregoing electrophysiological mapping, however, is an increased risk of suboptimal lead placement.[17-19] In this study, we sought to demonstrate a novel, automated method of electrophysiologically informed STN-DBS implantation that does not require the use of microelectrodes.

There is an increased interest in the use of oscillatory activity as a functional readout of STN entry and exit,[20] and previous studies of local field potential (LFP) activity derived from low-pass filtered MERs have demonstrated that the spatial extent of the STN could be characterized by increased oscillatory activity in the beta (13–30 Hz) frequency band[14,21-26] and/or high-frequency (>500 Hz) neuronal "noise."[27-29] The hypothesis of this study was that entry into and progression through the STN could be characterized by increased beta oscillatory activity measured from the DBS macroelectrodes directly. Dynamic (millimeter by millimeter) DBS macroelectrode recordings allow for the creation of a clinically relevant, LFP-based functional topology of the STN based on an established subthalamic neurophysiological marker. As such, the first objective of this study was to investigate whether DBS macrocontact recordings of beta-frequency activity could be used to intraoperatively guide lead placement. Moreover, because excessive beta-synchrony is suggested to be of pathophysiological relevance,[30] the second objective was to investigate whether this marker could be used for physiologically informed stimulation programming.

The benefits of an LFP-driven mapping approach are that the procedure can be automated and that the interpretation of the electrophysiological results may be more intuitive. Although such an approach may also be possible using MERs, the use of only the DBS macroelectrode may reduce the risk of hemorrhage and may also have time-savings and cost-saving benefits. A disadvantage of this approach compared with MER-guided procedures is that MERs can offer multiple simultaneous recording trajectories, thus increased information in the x and y planes. A disadvantage of electrophysiology guided approaches in general (LFP or MER) compared with image-guided only procedures is that the patient is usually awake; however, awake electrophysiology guided surgeries enable robust scrutiny of side effect thresholds during perioperative test stimulation and allow for the ability to make targeted implantations of stimulation contacts into different regions along the dorsal-ventral axis, such as placement of a stimulating contact into the zona incerta[31] or substantia nigra pars reticulata (SNr).[32] Thus, we suggest that the presented LFP-based DBS macroelectrode mapping procedure may be used as an alternative to or in conjunction with MER-guided procedures, with notable advantages compared with procedures that rely on image guidance only.

Methods

Patients and Lead Types

A total of 39 patients with Parkinson's disease were included in this study; 13 patients ($n_{hemispheres}$ = 26) received bilateral omnidirectional DBS leads (3389, Medtronic Inc, Minneapolis, MN) and 26 patients ($n_{hemispheres}$ = 52) received bilateral segmented DBS leads (6170, Abbott Laboratories, Lake Bluff, IL). The dorsal-most and ventral-most levels of the segmented leads contained omnidirectional contacts, whereas the 2 middle levels contained 3 segments each (frontal, medial, lateral). Each patient underwent DBS implantation after overnight withdrawal from antiparkinsonian medication, and there were no surgical complications to report. The study was approved by the ethics committee of the University Hospital Tübingen. Patient demographics are available in the Supplementary Material.

Surgical Procedures

In each patient, the tentative location of the STN was first determined radiologically.[33] The desired electrode depth in the STN region was determined by phenotype-specific clinical symptoms. In tremor-dominant patients, the tentative location of the dorsal-most contacts was at the upper border of the STN to stimulate the zona

incerta.[31] In patients with dominant gait and postural symptoms, the tentative location of the ventral-most contact was at the lower border of the STN to stimulate the SNr region.[32] Patients with segmented leads who did not fit either of the aforementioned criteria were implanted such that the levels with segmented contacts were within the STN to allow for the maximized potential of directional stimulation titration. Planning of the surgical trajectory/approach did not differ based on these distinct targets; rather, only the implantation depth was considered based on electrophysiological mapping.

In all 39 patients ($n_{hemispheres}$ = 78), recordings of the LFPs were obtained simultaneously from 4 to 8 monopolar macroelectrode recordings of omnidirectional or segmented lead contacts at every millimeter along the surgical trajectory. Measurements began with the bottom of ventral-most contact at 8 to 10 mm above the tentative target, and each subsequently dorsal contact level simultaneously recorded at +2 mm, +4 mm, and + 6 mm above, respectively.[34] At each depth, 30-second LFP recordings were simultaneously acquired from each contact, and the power spectral density (PSD) functions were obtained (details in section "Online LFP-based mapping: DBS macroelectrode recordings") and visualized online (as seen in Fig. 1). In 8 ($n_{hemispheres}$ = 16) of the 26 patients with segmented leads, MERs were performed (details in section "MER-based mapping: Microelectrode recordings") prior to DBS macroelectrode recordings.

Online LFP-Based Mapping: DBS Macroelectrode Recordings

Monopolar LFP recordings from each of the DBS contacts were sampled at ≥1200 Hz (hardware filter: 0.075 Hz–3.5 kHz) using an intraoperative recording device (NeuroOmega, Alpha Omega Engineering, Nof HaGalil, Israel). For online calculations of PSDs, 30-second LFP recordings were streamed from the NeuroOmega device (the streaming function is available via the NeuroOmega application programming interface) to an external personal computer. The LFP data were then transformed into the frequency domain using a multitaper approach (1 Hz frequency resolution) in Python 3.6 (Python Software Foundation, Fredericksburg, Virginia, USA; code available in the Supplementary Material). At each depth, PSDs were plotted and displayed immediately after calculation (as in Fig. 1). In cases where microelectrode recordings were not performed, the final position of the DBS lead was determined based on the presence and spatial extent of beta activity (with different depths used for the different desired functional outcomes, as explained previously). In the case of a complete lack of beta activity along the surgical trajectory, lead positioning relied on the results of perioperative test stimulation (eg, symptom reduction and adverse effects elicited by stimulation of nearby fiber pathways). If side effect thresholds were acceptable, the lead was positioned according to the radiologically defined target. If side effect thresholds were unacceptable, the DBS lead was repositioned and a second DBS LFP mapping trajectory was performed.

Post hoc statistical analyses of LFP data were also carried out using 2 separate methods (outlined in sections "Omnidirectional leads: Beta-peak depth spectrograms" and "Segmented leads: Beta-peak discretization"). One method involved reconstructing the distributions of spectral activity along surgical trajectories (done for patients with segmented leads), and the other method involved direct discretization (presence vs. lack) of beta activity (done for patients with segmented leads). The reason for using 2 separate data sets for the 2 different, although complementary, analyses was that this prevents overinflation of statistical power and prevents redundancy (ie, analyzing the same data set twice in 2 different ways). Moreover, the inclusion of patients with 2 different lead types was meant to demonstrate that the LFP-based DBS macroelectrode mapping approach could be applied regardless of electrode type/model.

Omnidirectional Leads: Beta-Peak Depth Spectrograms

For the 13 patients ($n_{hemispheres}$ = 26) with omnidirectional leads, 3-dimensional "depth spectrograms" (depth, frequency, power) were generated for each contact and for each hemisphere by normalizing beta-peak amplitudes with respect to the highest beta-peak amplitude recorded across all depths ($n_{hemispheres}$ = 21; we excluded 2 patients and a total of 5 hemispheres because of excessive noise or lack of beta peaks). This was done to generate a distribution of the spectral information across the surgical trajectory. This enables the visualization of the estimated spatial extent of the STN and demonstrates the reproducibility of measurements across successive contacts. A group depth spectrogram was generated by averaging the depth spectrograms of the ventral-most (or second-most ventral in case of strong artifacts) contact from each hemisphere ($n_{hemispheres}$ = 21) aligned at (1) the depth of the highest beta peak (y axis) and (2) the frequency of the highest beta peak (x axis). For each individual hemisphere, the mean squared error was calculated between the depth spectrogram of the ventral-most (or second-most ventral in case of strong artifacts) contact and a 3-dimensional Gaussian distribution, followed by a permutation test (100,000 permutations) to determine the significance of the mean squared error. This permutation test was also performed for the group depth spectrogram, except the peak voxel of each permutation was also centered. Postoperative imaging was performed with MRI and computed tomography in omnidirectional and segmented leads, respectively (further methodological details are available in Supplementary Material).[35] The MRI-

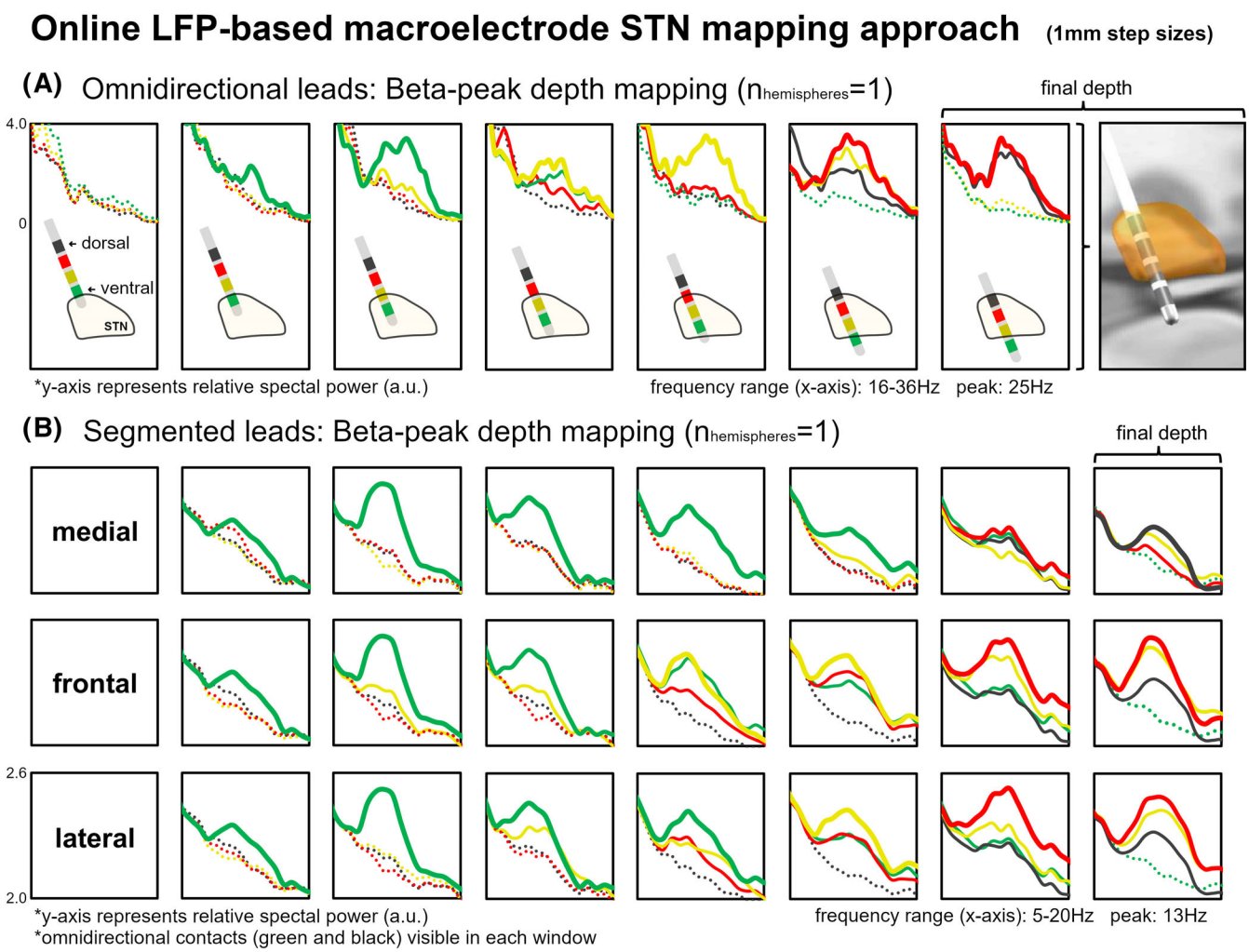

FIG. 1. Online local field potential–based macroelectrode STN mapping approach. Entry of each successive macrocontact into the STN was determined by sequential increases in beta power. (**A**) Sample recording trajectory from 1 hemisphere using an omnidirectional lead. Power spectral densitys at the final depth are corroborated by postoperative lead localization. (**B**) Sample recording trajectory from 1 hemisphere using a segmented lead. The power spectral density at the 2 omnidirectional contact levels (green ventral-most and black dorsal-most contacts) are displayed as duplicates in each of the directional windows (medial, frontal, lateral; which correspond to the 3 segmented contacts at the yellow second-most ventral and red second-most dorsal contact levels). STN, subthalamic nucleus. [Color figure can be viewed at wileyonlinelibrary.com]

based postoperative lead localizations could indeed corroborate intraoperative results (further examples are available in the Supplementary Material).

Segmented Leads: Beta-Peak Discretization

Of the 26 patients ($n_{hemispheres}$ = 52) with segmented leads, data from 8 patients ($n_{hemispheres}$ = 16) were used for corroboration with MER (discussed in the next section). For the other 18 patients ($n_{hemispheres}$ = 36), PSD measurements were used for LFP-based beta-peak discretization. For each hemisphere ($n_{hemispheres}$ = 27; we excluded 1 patient and a total of 9 hemispheres because of excessive noise or lack of beta peaks), the depth-normalized (subsequently subtracting 2 mm, 4 mm, and 6 mm from contacts dorsal to the ventral-most, respectively) beta-peak amplitudes at each contact were plotted along with the PSD amplitudes of nonpeaks (ie, background activity within the patient-specific beta-peak frequency range). To obtain a visualization of the group data, all individual hemispheres ($n_{hemispheres}$ = 27) were normalized (by dividing by the interdecile of the local nonpeak activity; data that come from the recording sites assumed to be outside, not within, the STN) and plotted together after alignment to the depth of the LFP-defined STN entry (ie, first depth at which a user-defined beta peak was detected by a deviation/increase with respect to "background" nonpeak activity). This method for analyzing data from segmented electrodes, which carries more information (ie, directional information), allows for the ability to discern both the depth and direction of the highest beta peak across the entire recording trajectory on a per-hemisphere basis in a condensed manner. For each hemisphere individually, as well as for the group data,

2-tailed *t* tests (unpaired) were used to differentiate the amplitudes of beta peaks from the amplitudes of nonpeak background activity.

MER-Based Mapping: Microelectrode Recordings

In 8 patients ($n_{hemispheres}$ = 16), LFP beta-peak mapping was corroborated by the MER of single-unit activity. Electrophysiological mapping of the STN and SNr using single-unit activity has been previously reported.[13,36] Briefly, STN neurons were identified by firing rates of ~20 to 60 Hz and irregular firing patterns, periods of beta activity, and responsiveness to passive movements of the contralateral extremities. After 4-mm to 6-mm advancement through the STN, exit from ventral border was identified by a reduction in background noise. After a brief quiescent period, SNr neurons were identified by faster firing rates of 80 to 120 Hz and regular firing patterns.

To corroborate the LFP-based beta-peak mapping approach, we compared the spatial characteristics of beta-peak appearance/disappearance ($n_{hemispheres}$ = 13; we excluded 3 hemispheres because of excessive noise or lack of beta peaks) along the surgical trajectories (1 mm step sizes) using the ventral-most contact with respect to the MER-defined STN entry and exit (submillimeter spatial resolution; ~0.1 mm step sizes). We defined the average depth of the first beta peak and the average depth of the highest beta peak with respect to the MER-defined STN entry. We also defined the average depth of the last beta

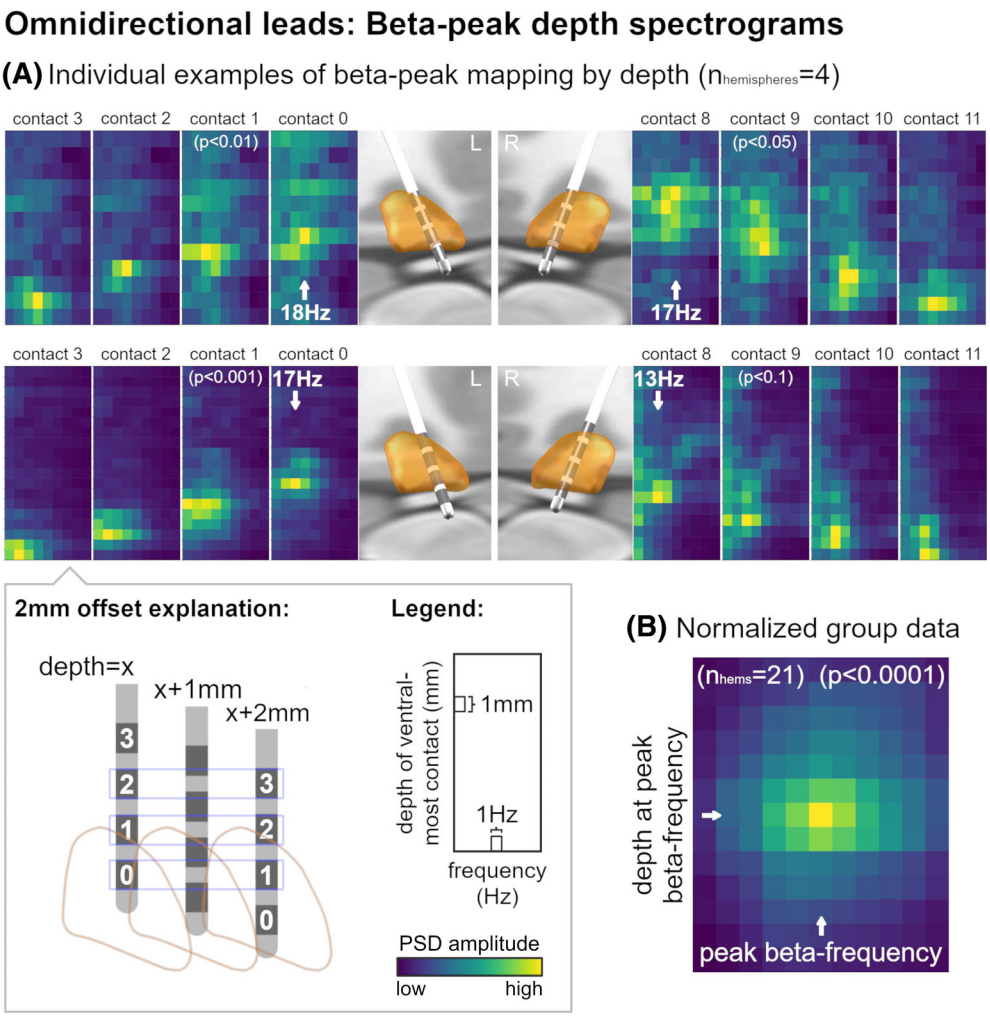

FIG. 2. Omnidirectional leads: beta-peak depth spectrograms. This approach allows for the visualization of the spatial-specificity of subthalamic nucleus beta-frequency activity across the surgical trajectory. (**A**) Individual examples (2 patients; $n_{hemispheres}$ = 4) of depth spectrograms and postoperative leads localizations. The 2-mm offsets are demonstrated in successive contact depth spectrograms from ventral to dorsal (ie, each successive contact records the same as the ventral-most contact after a 2 mm, 4 mm, and 6 mm advancements, respectively). The legend in the bottom left of this figure shows the depth (1 mm) and frequency (1 Hz) resolutions of the respective axes and also demonstrates the reason for the 2-mm offsets. In each of the 11 patients, the mean squared error of the beta-frequency depth spectrogram was significantly smaller compared with its permutations in 19 of 21 hemispheres (2 were P = 0.1–0.05, 6 were P = 0.05–0.01; 3 were P = 0.01–0.001; 8 were P < 0.001). (**B**) This was also confirmed at the group level ($n_{hemispheres}$ = 21; P < 0.0001). This group spectrogram was generated by normalizing with respect to the depth of the highest beta peak (*y*-axis) and the frequency of the beta peak (*x*-axis). PSD, power spectral density. [Color figure can be viewed at wileyonlinelibrary.com]

peak and the average depth of the first recording site at which the beta peak disappeared with respect to the MER-defined STN exit.

Clinical Relevance of Beta-Peak Amplitudes at Final Implantation Site

To determine if beta-peak amplitudes measured at the final implantation site had clinical relevance, we calculated how often the lead was programmed to stimulate at the same level at which the highest beta-peak amplitude was measured (26 patients; $n_{hemispheres}$ = 45; the total number of hemispheres with viable electrophysiological data and who were not tremor dominant). Tremor-dominant patients (9 patients; $n_{hemispheres}$ = 18) were excluded as these patients were most often programmed on the dorsal-most contacts to stimulate the zona incerta (outside of the STN). For segmented leads, the contacts at each segmented level were averaged together to get the average beta-peak amplitude for that level. Lead programming was done using a standard monopolar review ≥8 weeks after surgery, and the clinician was blinded with respect to the LFP results. If bipolar stimulation was programmed ($n_{hemispheres}$ = 11), a match was considered if 1 of the bipolar contacts was the contact with highest beta peak.

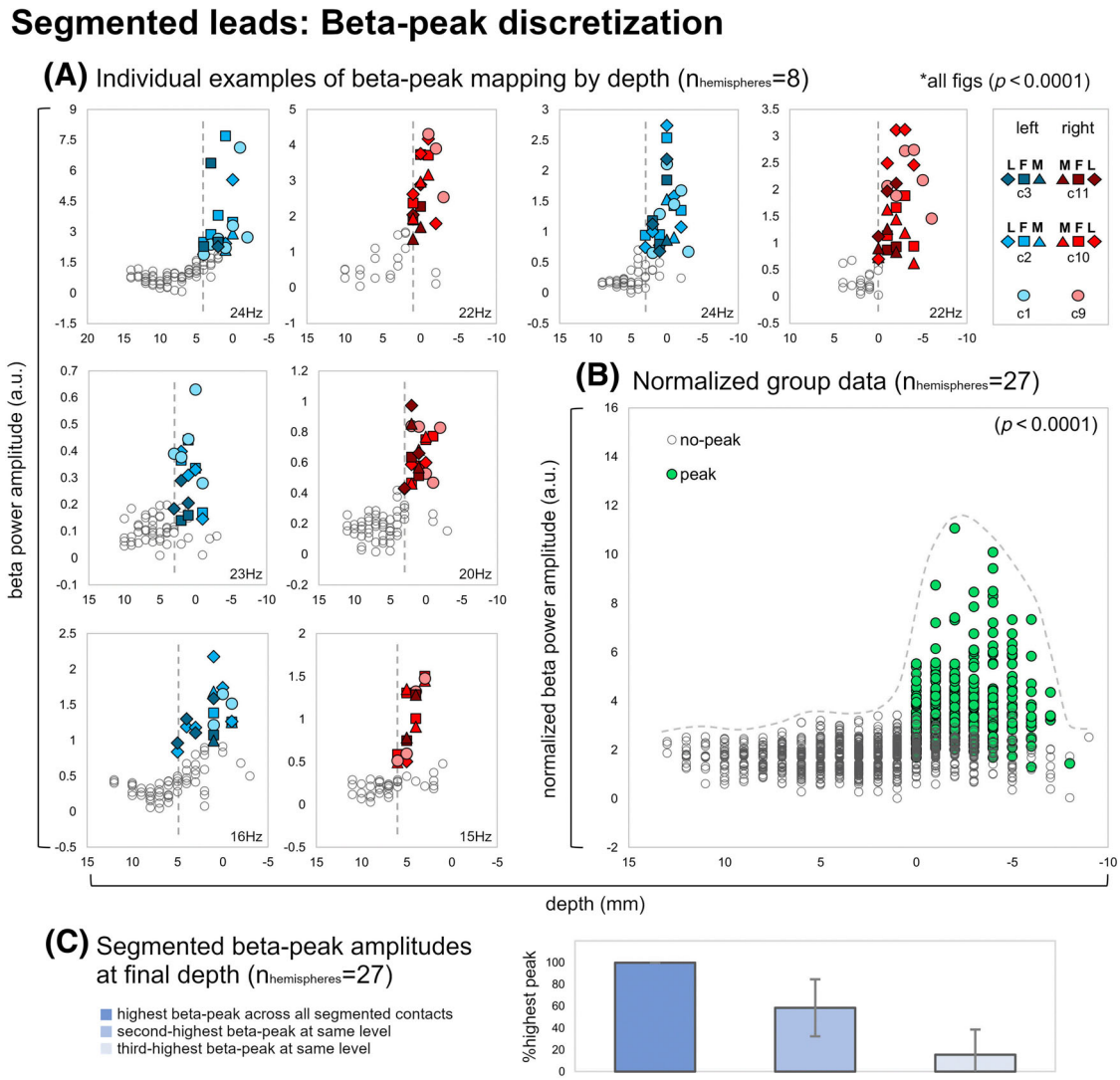

FIG. 3. Segmented leads: beta-peak discretization. Beta-peak amplitudes at recording sites presumed to be within the subthalamic nucleus were significantly greater than at sites not within the subthalamic nucleus. (**A**) Individual examples (4 patients; $n_{hemispheres}$ = 8) of beta-peak amplitudes plotted by depth. The depth of each contact was normalized with respect to the ventral-most contact (by subtracting 2 mm, 4 mm, and 6 mm from the second-most ventral, second-most dorsal, and dorsal-most contact levels, respectively). In each of 17 patients, when considering hemispheres individually ($n_{hemispheres}$ = 27), subthalamic nucleus beta peaks could be robustly differentiated from nonpeaks ($P < 0.0001$). The beta-peak frequency is displayed in the bottom right corner of each plot. (**B**) The same was true for the normalized group ($n_{hemispheres}$ = 27) data ($P < 0.0001$). Beta-peak amplitude normalization was done by dividing by the range of the background noise (ie, nonpeak activity), and depth normalization was done by assigning depth 0 to the recording site of the first beta peak. (**C**) At the final implantation sites, the highest beta-peak amplitude across all segmented contacts was considered as 100%. The average amplitudes (± standard deviation) of the second-highest and third-highest beta peaks at the same level are shown, normalized to the highest peak. F, frontal; L, lateral; M, medial. [Color figure can be viewed at wileyonlinelibrary.com]

Results

Online LFP-Based Mapping: DBS Macroelectrode Recordings

We applied the LFP-based mapping approach in 78 hemispheres; in 16 of these hemispheres, microelectrode recordings were performed beforehand and used to determine the final trajectories of the DBS leads. In 47 of the remaining 62 hemispheres, the LFP physiology decided the final lead positioning. In the remainder, intraoperative test stimulation (symptom suppression, reasonable side effect thresholds) determined the final trajectories. In most of these cases, lead repositioning was not required, and electrodes were implanted at the radiologically defined target sites. In 2 hemispheres (outlined in the patient demographics table in the Supplementary Material), a second macroelectrode trajectory was performed, which each time yielded desirable electrophysiological results. From patients in whom postoperative MRI imaging was available, 2 examples of comparisons between LFP physiology and postoperative lead reconstruction are presented in Figure 2, and additional examples are available in the Supplementary Material.

Omnidirectional Leads: Beta-Peak Depth Spectrograms

Using PSD amplitudes in the beta-frequency band, 2 unique methods were employed to visualize and statistically differentiate STN recording sites from non-STN recording sites. The first method was to generate a spectral distribution of the patient-specific beta peak along the surgical trajectory; this was done for patients with omnidirectional leads. In 19 of 21 hemispheres (11 patients), the mean squared error of the beta-frequency depth spectrogram was significantly smaller compared with its permutations (2 were $P = 0.1–0.5$, 6 were $P < 0.05–0.01$, 3 were $P = 0.01–0.001$, 8 were $P < 0.001$; Fig. 2A). This indicates that, for most hemispheres, the depth spectrogram resembled a Gaussian

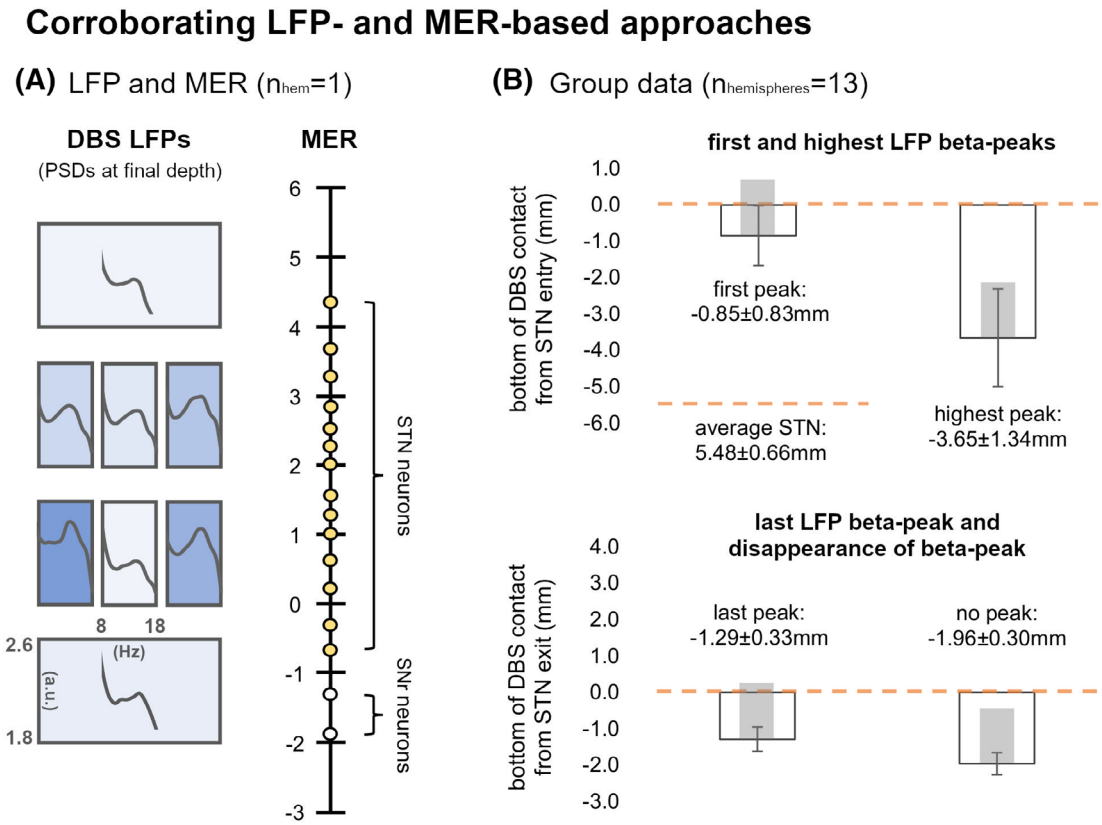

FIG. 4. Corroborating LFP-based and MER-based approaches. The macroelectrode LFP-based mapping approach was corroborated by the conventional MER-based mapping approach in 8 patients. (**A**) Displayed are the PSD amplitudes for each contact at the final implantation site (left) and the results from MER mapping of single unit activity along the surgical trajectory (right) from 1 representative hemisphere. Color gradient on DBS electrode contacts represents the relative beta-peak amplitude across contacts (ie, darkest blue being the highest peak and white being the lowest peak or no peak). (**B**) Group data ($n_{hemispheres} = 13$) demonstrates the average locations (± standard deviation) of the first detected beta peak and the highest beta peak with respect to the MER-defined STN entry (orange dashed line; top) as well as the locations of the last detected beta peak and the first location of the disappearance of the beta peak with respect to the MER-defined STN exit (orange dashed line; bottom). The depth at which each LFP measurement was obtained corresponds to the position of the bottom of the DBS macrocontact. The translucent gray rectangle in each bar represents the spatial extent of the DBS contact (1.5 mm). The group data suggest that a beta peak could be detected as long as a portion of the DBS macrocontact was within the MER-defined STN boundaries. DSB, deep brain stimulation; LFP, local field potential; MER, microelectrode recording; PSD, power spectral density; SNr, substantia nigra pars reticulata; STN, subthalamic nucleus. [Color figure can be viewed at wileyonlinelibrary.com]

distribution. This was confirmed at the group level ($n_{hemispheres}$ = 21; $P < 0.0001$; Fig. 2B).

Segmented Leads: Beta-Peak Discretization

The second method was to discretize the amplitudes of beta peaks at depths assumed to be within the STN from PSD amplitudes of background noise; this was done for patients with segmented leads. Beta-peak amplitudes at recording sites presumed to be within the STN were significantly greater than PSD amplitudes at recording sites not within the STN. This method provided additional direction-specific information (ie, which segmented contacts contained the highest amplitude beta peaks). When considering each hemisphere individually ($n_{hemispheres}$ = 27; 17 patients), STN beta peaks could be robustly differentiated from nonpeaks ($P < 0.0001$; Fig. 3A), and the same was true for the normalized group data ($P < 0.0001$;

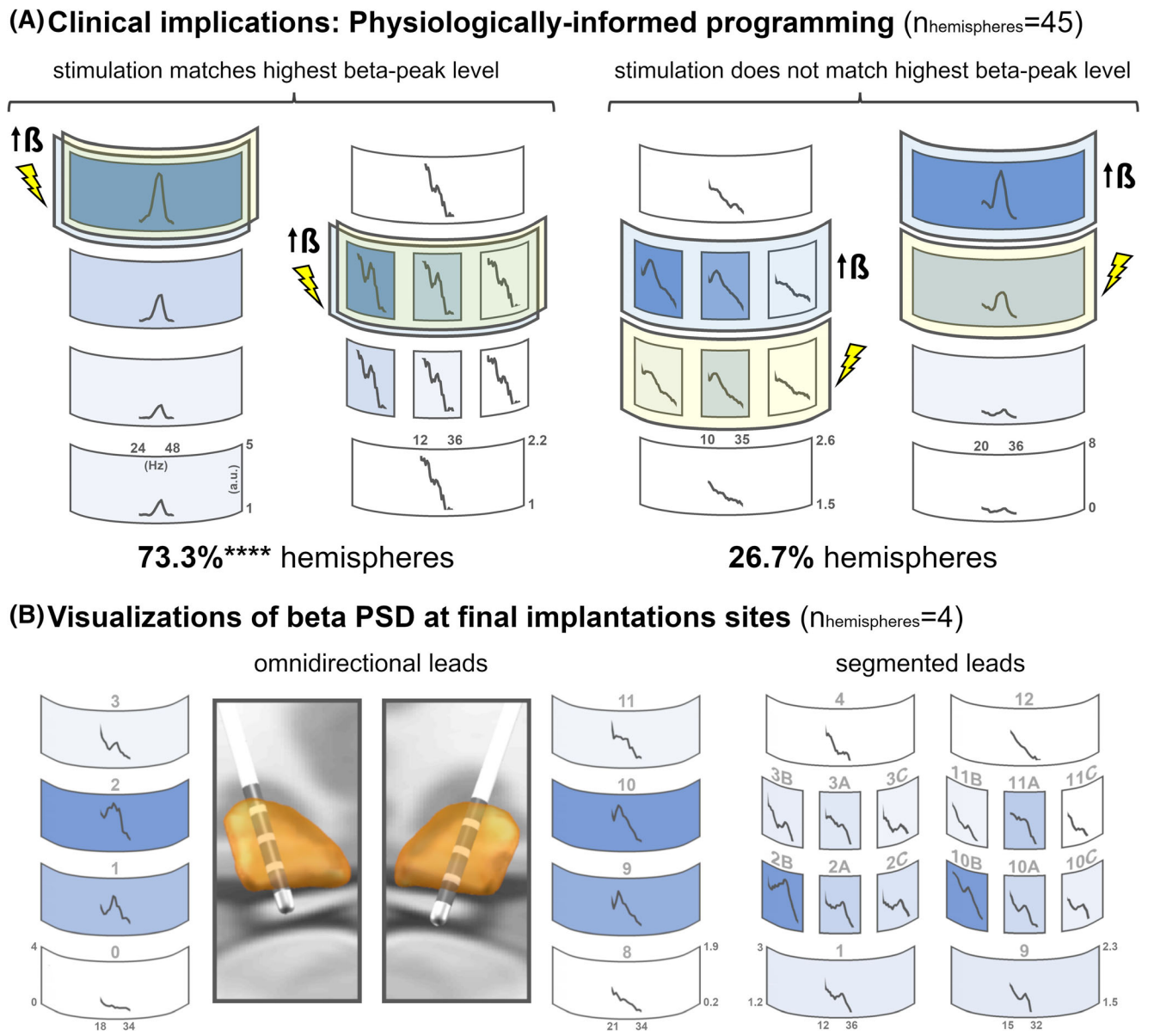

FIG. 5. Clinical implications: physiologically informed programming. (**A**) The macrocontact level with the highest beta-peak amplitude corresponded to the site of active stimulation (results of blinded monopolar reviews) 73.3% (33/45) of the time (26 patients; $n_{hemispheres}$ = 45). Of the remaining 26.7% (12/45), 75.0% (9/12) were programmed at the level of the second highest beta peak. Thus, the site of active stimulation was at either the highest or second-highest beta-peak level 93.3% (42/45) of the time. Tremor-dominant patients were excluded from this analysis. The displayed data are representative examples from 4 separate patients (4 hemispheres). (**B**) Additional representative examples of beta PSDs plotted on each of the deep brain stimulation macrocontacts at the final implantation sites for 1 patient with omnidirectional leads and another patient with segmented leads. Color gradients on DBS electrode contacts represent the relative beta-peak amplitudes across contacts per hemisphere (ie, darkest blue being the highest peak and white being the lowest peak or no peak). PSD, power spectral density. ****$P < 0.0001$. [Color figure can be viewed at wileyonlinelibrary.com]

Fig. 3B). Of the 62 hemispheres from 31 patients originally included in these analyses, statistically significant LFP-based electrophysiological STN delineation was achieved in 46 hemispheres (74.2%).

Corroborating LFP-Mapping and MER-Based Mapping Approaches

In the 8 patients in whom MER ($n_{hemispheres}$ = 16) and PSD measurements ($n_{hemispheres}$ = 13) were obtained, our results suggest that a detectable peak was measured when some portion of the DBS macrocontact was within the STN. Specifically, beta peaks first appeared when the bottom of the DBS contact was on average 0.85 ± 0.83 mm (mean ± standard deviation) beyond the MER-defined dorsal border (ie, when slightly more than half of the macrocontact had entered the STN). The largest peak was found when the bottom of the DBS contact was on average 3.65 ± 1.34 mm beyond the MER-defined border. Beta peaks were still visible when the bottom of the DBS macrocontact was an average of 1.29 ± 0.33 mm beyond the MER-defined ventral STN border (ie, when the majority of the DBS macrocontact had exited the STN but a small portion remained within). Beta peaks were no longer visible once the bottom of the DBS macrocontact was an average of 1.96 ± 0.30 mm beyond the ventral STN border. The average MER-defined spatial extent of STN was 5.48 ± 0.66 mm. These results are summarized in Figure 4.

Using data from all LFP-based mapping procedures ($n_{hemispheres}$ = 61), it was determined that the highest beta-peak amplitude was located 2.31 ± 1.6 mm beyond the area of first detectable beta peak (LFP-defined approach). Adjusting this value to account for the difference between MER-defined and LFP-defined dorsal border entry (ie, 0.85 ± 0.83 mm) confirms that the highest macroeletrode-defined beta peak was found when the bottom of the DBS contact was ~3.16 mm beyond the MER-defined STN border, which corroborates the aforementioned result of the highest beta-peak location.

Clinical Relevance of Beta-Peak Amplitudes at Final Implantation Site

The contact level with the highest beta-peak amplitude matched the clinically applied stimulation contact in 73.3% (33/45) of eligible hemispheres (Fig. 5A). Of the remaining 26.7% (12/45), 75% (9/12) were programmed at the level of the second-highest beta peak, whereas the remainder (3/12) were programmed at the dorsal-most contact level (which was neither the highest nor second-highest beta peak). This means that the site of active stimulation was at either the highest or second-highest beta-peak level 93.3% (42/45) of the time. Of the hemispheres, 2/3 that where neither at the highest nor second highest belonged to a single bilaterally mismatched patient who happened to be an equivalence-type patient who was programmed at the dorsal-most contacts on both sides for tremor benefit; contacts that were likely mostly outside of the STN as determined by a lack of beta peaks. If we exclude this patient, the active site of stimulation was at the highest beta-peak level 76.7% (33/43) of the time and at the level of the highest or second-highest peak 97.7% (42/43) of the time. If we consider that the maximum number of contacts that can simultaneously be in the STN is 3 (which covers a span of 5.5 mm), the match rate (73.3–76.7%) was more than 2-fold greater than chance (33.3%) and was statistically significant ($P < 0.0001$; binomial test).

Discussion

This study sought to demonstrate the instantaneous surgical and subsequent clinical relevance of subthalamic beta oscillations by applying a novel technique of functional mapping during DBS implantation procedures. The presented LFP-based method of electrophysiologically informed STN-DBS implantation required little time and fewer components (ie, use of the DBS macroelectrode only) and offered the possibility for semi-automation. We presented an online method (Fig. 1) for the intraoperative visualization and detection of the physiological STN topography based on PSD amplitudes in the beta-frequency band and presented 2 approaches for summary and statistical analysis of the results. One approach was to generate a distribution of beta-specific spectral information across the entire recording trajectory (Fig. 2), whereas the other approach was to discretize STN beta peaks from background activity (Fig. 3). In addition to describing the surgical functional utility of a beta-driven mapping approach, we also described a potentially promising technique for pathophysiologically informed stimulation programming (Fig. 5A). We suggest that delivering electrical stimulation from the macroelectrode contacts with the highest beta power at the final implantation site may yield the most favourable therapeutic results, which is corroborated by studies that suggest a relationship between subthalamic beta oscillations and clinical features of Parkinson's disease.

Surgical Utility: Electrophysiological Mapping

Improved imaging capabilities have led to the reconsideration of the use of electrophysiological mapping procedures.[37] Other arguments in support of omitting electrophysiological mapping procedures include reduced surgical time (thus, increased surgical tolerability) and reduced perioperative complications such as hemorrhage (although the risk rate is quite low at 3.3% for hematoma of any type, and 0.6% for symptomatic hematoma[38]).

However, neither high-resolution[39] nor conventional[40] imaging can account for perioperative deviations from preoperative anatomical targeting such as brain-shift,[41] which often contribute to suboptimal DBS lead placements.[42] Such deviations can only be accounted for when electrophysiological mapping procedures are correctly employed. Thus, we aimed to provide a novel methodology that can account for the majority of the aforementioned microelectrode contraindications while still providing a means of performing essential electrophysiologically informed implantations.

Given the unexpectedly high rate of DBS surgeries requiring lead revision or removal,[8] it can be argued that awake electrophysiology-guided implantations may be in the best interest of patients in the long term if corrective procedures can be avoided. Electrophysiological mapping procedures can reduce the likelihood of subsequent corrective surgeries, reduce the risk of surgical complications from subsequent procedures, and maximize therapeutic potential through optimized lead placement.[6] The approach described here furthermore reduces the necessity of expertise required for interpretation of MERs, can be performed rather quickly (barring technical or procedural obstacles, a 15-mm surgical trajectory takes only ~11 minutes; 30-second recordings at each depth and 15 seconds between depths) and eliminates time consumption associated with performing MERs. In addition, the risk of perioperative surgical complications (such as hemorrhage) from multipass microelectrode trajectories may be reduced. The described method furthermore allows for permutation of contact positions in accordance with patients' individual functional goals, such as placing the dorsal-most contact into the zona incerta to maximize effects on tremor,[31] placing the ventral-most contact into the SNr to potentially modulate gait dysfunction,[32] and/or placing segmented contacts into the STN to maximize the therapeutic window of STN-DBS.[43] Although z-direction titration is also possible with MERs, a particular advantage of the DBS macroelectrode approach is that once the optimal spot is determined based on electrophysiological results, the electrode stays in that spot chronically, whereas with MERs, the microwires must be removed and subsequently replaced by the chronic lead, which might introduce additional inaccuracies. As such, the DBS macrocontact approach may even serve as a final check to confirm that the DBS electrode is in place after replacing the microwire (ie, performing a DBS macroelectrode recording at the final position), thus the approach may also be used in conjunction with the traditional MER approach.

Two studies have previously applied a similar but distinct DBS macroelectrode mapping approach in smaller patient cohorts (n = 9[44] and n = 6[45]). The major difference is that both of these studies applied bipolar derivations of LFP recordings for offline spectral analyses. When 2 macrocontacts are both within the STN, bipolar recordings may lead to partial signal cancellation. Thus, for this application, bipolar recordings suffer from a nonstationary reference that leads to an inherent bias that shifts the location of the areas with highest beta activity to border regions where 1 contact is within the STN while another is outside of the STN. Conventional MER systems may also be configured such that the tip of the microelectrode is referenced to the macrotip located 3 mm dorsally, and each of these components are advanced together along the surgical trajectory (ie, a nonstationary reference). Monopolar recordings, as employed here, have a fixed reference and have the ability to create a functional topography of beta activity both within and outside of the STN without the bias of a moving reference. Although bipolar recordings may limit the effects of volume conduction,[46] our results nevertheless demonstrate the viability of using monopolar recordings for electrophysiological mapping and moreover suggest that the region of highest beta activity may not necessarily be at the immediate border region (although monopolar LFP recordings using microelectrodes would provide greater spatial acuity for assessing this).

Surgical Utility: Considerations and Limitations

Based on the results of corroboration with conventional MER-based mapping, offsets between LFP-defined and MER-defined borders should be taken into consideration, namely, that a beta peak may be visible if any portion of the DBS macrocontact is within the STN. Other considerations while performing these online recordings include that the patient should keep voluntary movements (which can desynchronize beta activity and/or induce movement artifacts) to a minimum, should not be speaking, and should be awake/alert. Because these behaviors are sometimes unavoidable, measurements at a particular depth may need to be repeated. Patients should be *off* medication, as antiparkinsonian medications have been shown to attenuate beta oscillations.[47] Furthermore, this method has not yet been confirmed in patients operated on under general anesthesia (which has effects on neuronal activity[48]). In this study, we could visualize and delineate STN from non-STN recording sites in 76.7% of hemispheres. However, a particularly important limitation of this approach is that some patients may lack beta activity[49] (also described in parkinsonian primate models[50]). In such cases, lead placements must rely on preoperative imaging and planning as well as results from perioperative test stimulation. However, in the event that both electrophysiological and perioperative test stimulation results are not favorable, an additional macroelectrode trajectory may have to be performed. Although this circumstance is not ideal, it still enables the ability to perform an electrophysiologically informed corrective trajectory on the spot, whereas an asleep image-guided-only procedure may result in a chronic lead misplacement that would necessitate a subsequent corrective procedure at a later date. In this regard,

the advantage of MERs is that they can enable performing multiple simultaneous recording trajectories, thus generating more information in the anterior–posterior and medial–lateral planes prior to macroelectrode implantation. Segmented leads may be able to provide some additional directional information in these planes as well in the fact that the distance between centroids of the directional contacts is 1.22 mm (compared with the 2 mm between MER trajectories adjacent to the central track). Thus, if perioperative test stimulation returns suboptimal side effect thresholds, but 1 of the directional contacts may have a small beta peak in 1 particular direction (and no peaks at all in the other directions), this may inform the direction for a potential revised trajectory. Finally, a notable limitation of electrophysiologically informed surgeries altogether is that they usually require that the patient be awake, unlike image-guided-only surgeries; however, awake surgeries allow for the ability to test for sensory-related adverse effects (ie, stimulation of lemniscus fibers) or behavioral-related adverse effects (ie, speech effects from stimulation of cortico-bulbar fibers).

Clinical Utility: Stimulation Programming

Subthalamic hypersynchrony in the beta-frequency band has been suggested to be associated with clinical features of Parkinson's disease.[30,51-54] In addition, both levodopa therapy[14,47,55] and STN-DBS,[56-58] the conventional therapeutic interventions for Parkinson's disease, have been suggested to disrupt/desynchronize these purportedly pathological oscillations. As such, we postulated that targeted stimulation delivery to the area of highest beta-peak amplitude may be most therapeutically favorable. We investigated this by comparing the macrocontact level with the highest intraoperatively obtained beta-peak amplitude at the final implantation site to the eventual programmed stimulation site determined during conventional postoperative monopolar review that was blinded to the intraoperative LFP results and found a high degree of correspondence (Fig. 5A). A previous study (n = 128) demonstrated that the spatial extent of the subthalamic beta oscillatory region was a predictor of favorable therapeutic response.[21] Furthermore, a study in patients (n = 4) programmed with bipolar stimulation found that the contact pair that provided optimal efficacy was associated with the highest energy in the beta and gamma frequency bands.[59] Another study applied this approach of beta-targeted stimulation in patients (n = 12) implanted with directional leads.[49] The authors found that the beta power at each contact was correlated with the individual contact's clinical efficacy and that 1 of the 2 contacts with the highest beta power was the most clinically efficient stimulation contact up to 92% of the time, which corresponds with our findings.

Previous studies as well as our own suggest that stimulation programming can be optimized not only to reduce time consumption associated with conducting a complete monopolar review but also to be performed in a physiologically informed manner. As such, we suggest that novel implantable pulse generator software and hardware should include the capability for the clinician to quickly record (eg, for 30 seconds) from each of the macrocontacts of the embedded DBS leads, calculate and display the PSDs (as shown in Fig. 5B), and give the option to the clinician to select stimulation contacts based on the amplitude of PSDs (as shown in Fig. 5A). This is additionally important considering the emergence of segmented DBS leads with many contacts and considering the variability in beta-peak amplitude across directional contacts (Fig. 3C). Although suggested to be able to widen the therapeutic window,[43,60] stimulation programming will become much more cumbersome and time consuming. We foresee that physiologically informed stimulation programming will be feasible in the near future considering the emergence of DBS technologies with chronic sensing capabilities. Thus, studies of macroelectrode LFP signals have the potential for direct technological and clinical translation.

Clinical Utility: Considerations and Limitations

Consistent with previous findings,[29] beta oscillations could still be measured in the subgroup of tremor-dominant patients. For these patients, however, the clinically applied contact was usually not the one with the highest beta activity because of the intended stimulation in the zona incerta, that is, above the dorsal STN border. In nontremor dominant patients, the potential reasons for mismatches between the contact with the highest beta-peak amplitude and the clinically applied stimulation contact level are (1) a narrow therapeutic window at the contact with the highest beta peak because of proximity to the nearby fibers or (2) selection of therapeutically suboptimal active stimulation contacts.[61] Nevertheless, the active contacts corresponded to the level of the first-highest or second-highest beta-peak amplitude in 93.3% of hemispheres, thereby emphasizing the clinical functional utility of this physiological marker. Although it would be valuable to assess the relevance of beta activity recorded with individual segmented contacts for informing directional stimulation, systematic clinical assessments (monopolar review) of directional stimulation titration were not performed in this patient cohort. As such, further clinical research is warranted to determine if beta-peak amplitude could inform directional stimulation programming.

Conclusion

We demonstrated the feasibility of performing an online LFP-based, beta-driven electrophysiological mapping procedure using DBS macroelectrodes. Furthermore, our results suggest that the PSD in the beta-frequency band at

the final implantation site may be used for physiologically informed stimulation delivery. As such, our results demonstrate both surgical and clinical functional utilities of beta oscillations measured from DBS macroelectrodes. These findings may be used to improve both surgical implantation and stimulation programming procedures.

Acknowledgments: We thank Dr. Ramin Azodi-Avval for his contributions to data collection and the patients for their participation in the study.

References

1. Limousin P, Krack P, Pollak P, et al. Electrical stimulation of the subthalamic nucleus in advanced Parkinson's disease. N Engl J Med 1998;339:1105–1111. https://doi.org/10.1056/NEJM199810153391603
2. Benabid AL, Pollak P, Gross C, et al. Acute and long-term effects of subthalamic nucleus stimulation in Parkinson's disease. Stereotact Funct Neurosurg 1994;62:76–84. https://doi.org/10.1159/000098600
3. Vitek JL. Deep brain stimulation for Parkinson's disease. Stereotact Funct Neurosurg 2002;78:119–131. https://doi.org/10.1159/000068959
4. Farris S, Giroux M. Retrospective review of factors leading to dissatisfaction with subthalamic nucleus deep brain stimulation during long-term management. Surg Neurol Int 2013;4:69. https://doi.org/10.4103/2152-7806.112612
5. Hariz MI. Complications of deep brain stimulation surgery. Mov Disord 2002;17:S162–S166. https://doi.org/10.1002/mds.10159
6. Lozano AM, Snyder BJ, Hamani C, et al. Basal ganglia physiology and deep brain stimulation. Mov Disord 2010;25:S71–S75. https://doi.org/10.1002/mds.22714
7. Nickl RC, Reich MM, Pozzi NG, et al. Rescuing suboptimal outcomes of subthalamic deep brain stimulation in Parkinson disease by surgical lead revision. Neurosurgery 2019;85:E314–E321. https://doi.org/10.1093/neuros/nyz018
8. Rolston JD, Englot DJ, Starr PA, et al. An unexpectedly high rate of revisions and removals in deep brain stimulation surgery: analysis of multiple databases. Parkinsonism Relat Disord 2016;33:72–77. https://doi.org/10.1016/j.parkreldis.2016.09.014
9. Okun MS, Tagliati M, Pourfar M, et al. Management of referred deep brain stimulation failures: a retrospective analysis from 2 movement disorders centers. Arch Neurol 2005;62:1250–1255. https://doi.org/10.1001/archneur.62.8.noc40425
10. Moro E, Esselink RJA, Xie J, et al. The impact on Parkinson's disease of electrical parameter settings in STN stimulation. Neurology 2002;59:706–713. https://doi.org/10.1212/wnl.59.5.706
11. Witt K, Daniels C, Volkmann J. Factors associated with neuropsychiatric side effects after STN-DBS in Parkinson's disease. Parkinsonism Relat Disord 2012;18:S168–S170. https://doi.org/10.1016/S1353-8020(11)70052-9
12. Brunenberg EJL, Platel B, Hofman PAM, et al. Magnetic resonance imaging techniques for visualization of the subthalamic nucleus: a review. J Neurosurg 2011;115:971–84. https://doi.org/10.3171/2011.6.JNS101571
13. Hutchison WD, Allan RJ, Opitz H, et al. Neurophysiological identification of the subthalamic nucleus in surgery for Parkinson's disease. Ann Neurol 1998;44:622–628. https://doi.org/10.1002/ana.410440407
14. Weinberger M, Mahant N, Hutchison WD, et al. Beta oscillatory activity in the subthalamic nucleus and its relation to dopaminergic response in Parkinson's disease. J Neurophysiol 2006;96:3248–3256. https://doi.org/10.1152/jn.00697.2006
15. Abosch A, Hutchison WD, Saint-Cyr JA, et al. Movement-related neurons of the subthalamic nucleus in patients with Parkinson disease. J Neurosurg 2002;97:1167–1172. https://doi.org/10.3171/jns.2002.97.5.1167
16. Lee PS, Crammond DJ, Richardson RM. Deep brain stimulation of the subthalamic nucleus and globus pallidus for Parkinson's disease. Curr Concepts Mov Disord Manag 2018;33:207–221. https://doi.org/10.1159/000481105
17. Montgomery EB. Microelectrode targeting of the subthalamic nucleus for deep brain stimulation surgery. Mov Disord 2012;27:1387–1391. https://doi.org/10.1002/mds.25000
18. Lozano CS, Ranjan M, Boutet A, et al. Imaging alone versus microelectrode recording–guided targeting of the STN in patients with Parkinson's disease. J Neurosurg 2018;130:1847–1852. https://doi.org/10.3171/2018.2.JNS172186
19. Bour LJ, Contarino MF, Foncke EMJ, et al. Long-term experience with intraoperative microrecording during DBS neurosurgery in STN and GPi. Acta Neurochir (Wien) 2010;152:2069–2077. https://doi.org/10.1007/s00701-010-0835-y
20. Valsky D, Marmor-Levin O, Deffains M, et al. Stop! border ahead: automatic detection of subthalamic exit during deep brain stimulation surgery. Mov Disord 2017;32:70–79. https://doi.org/10.1002/mds.26806
21. Zaidel A, Spivak A, Grieb B, et al. Subthalamic span of β oscillations predicts deep brain stimulation efficacy for patients with Parkinson's disease. Brain 2010;133:2007–2021. https://doi.org/10.1093/brain/awq144
22. Shamir RR, Zaidel A, Joskowicz L, et al. Microelectrode recording duration and spatial density constraints for automatic targeting of the subthalamic nucleus. Stereotact Funct Neurosurg 2012;90:325–334. https://doi.org/10.1159/000338252
23. Alavi M, Dostrovsky JO, Hodaie M, et al. Spatial extent of beta oscillatory activity in and between the subthalamic nucleus and substantia nigra pars reticulata of Parkinson's disease patients. Exp Neurol 2013;245:60–71. https://doi.org/10.1016/j.expneurol.2012.09.021
24. Kolb R, Abosch A, Felsen G, et al. Use of intraoperative local field potential spectral analysis to differentiate basal ganglia structures in Parkinson's disease patients. Physiol Rep 2017;5:e13322. https://doi.org/10.14814/phy2.13322
25. Thompson JA, Oukal S, Bergman H, et al. Semi-automated application for estimating subthalamic nucleus boundaries and optimal target selection for deep brain stimulation implantation surgery. J Neurosurg 2018;1:1–10. https://doi.org/10.3171/2017.12.JNS171964
26. Kühn AA, Trottenberg T, Kivi A, et al. The relationship between local field potential and neuronal discharge in the subthalamic nucleus of patients with Parkinson's disease. Exp Neurol 2005;194:212–220. https://doi.org/10.1016/j.expneurol.2005.02.010
27. Novak P, Daniluk S, Ellias SA, et al. Detection of the subthalamic nucleus in microelectrographic recordings in Parkinson disease using the high-frequency (> 500 Hz) neuronal background: technical note. J Neurosurg 2007;106:175–179. https://doi.org/10.3171/jns.2007.106.1.175
28. Telkes I, Jimenez-Shahed J, Viswanathan A, et al. Prediction of STN-DBS electrode implantation track in Parkinson's disease by using local field potentials. Front Neurosci 2016;10:198. https://doi.org/10.3389/fnins.2016.00198
29. Telkes I, Viswanathan A, Jimenez-Shahed J, et al. Local field potentials of subthalamic nucleus contain electrophysiological footprints of motor subtypes of Parkinson's disease. Proc Natl Acad Sci 2018;115:E8567–E8576. https://doi.org/10.1073/pnas.1810589115
30. Brown P. Oscillatory nature of human basal ganglia activity: relationship to the pathophysiology of Parkinson's disease. Mov Disord 2003;18:357–63. https://doi.org/10.1002/mds.10358
31. Plaha P, Khan S, Gill SS. Bilateral stimulation of the caudal zona incerta nucleus for tremor control. J Neurol Neurosurg Psychiatry 2008;79:504–513. https://doi.org/10.1136/jnnp.2006.112334
32. Weiss D, Walach M, Meisner C, et al. Nigral stimulation for resistant axial motor impairment in Parkinson's disease? A randomized controlled trial. Brain 2013;136:2098–2108. https://doi.org/10.1093/brain/awt122
33. Bejjani B-P, Dormont D, Pidoux B, et al. Bilateral subthalamic stimulation for Parkinson's disease by using three-dimensional stereotactic magnetic resonance imaging and electrophysiological guidance.

J Neurosurg 2000;92:615–25. https://doi.org/10.3171/jns.2000.92.4.0615

34. Azodi-Avval R, Gharabaghi A. Spatial specificity of beta oscillations and cortico-subthalamic connectivity in Parkinson's disease [doctoral thesis]. Tuebingen, Germany: University of Tuebingen; 2018.
35. Horn A, Li N, Dembek TA, et al. Lead-DBS v2: towards a comprehensive pipeline for deep brain stimulation imaging. NeuroImage 2019;184:293–316. https://doi.org/10.1016/j.neuroimage.2018.08.068
36. Milosevic L, Kalia SK, Hodaie M, et al. Neuronal inhibition and synaptic plasticity of basal ganglia neurons in Parkinson's disease. Brain 2018;141:177–190. https://doi.org/10.1093/brain/awx296
37. Foltynie T, Zrinzo L, Martinez-Torres I, et al. MRI-guided STN DBS in Parkinson's disease without microelectrode recording: efficacy and safety. J Neurol Neurosurg Psychiatry 2011;82:358–363. https://doi.org/10.1136/jnnp.2010.205542
38. Binder DK, Rau GM, Starr PA. Risk factors for hemorrhage during microelectrode-guided deep brain stimulator implantation for movement disorders. Neurosurgery 2005;56:722–732. https://doi.org/10.1227/01.NEU.0000156473.57196.7E
39. Cho Z-H, Min H-K, Oh S-H, et al. Direct visualization of deep brain stimulation targets in Parkinson disease with the use of 7-tesla magnetic resonance imaging: clinical article. J Neurosurg 2010;113:639–647. https://doi.org/10.3171/2010.3.JNS091385
40. Ranjan M, Boutet A, Xu DS, et al. Subthalamic nucleus visualization on routine clinical preoperative MRI scans: a retrospective study of clinical and image characteristics predicting its visualization. Stereotact Funct Neurosurg 2018;96:120–126. https://doi.org/10.1159/000488397
41. Halpern CH, Danish SF, Baltuch GH, et al. Brain shift during deep brain stimulation surgery for Parkinson's disease. Stereotact Funct Neurosurg 2008;86:37–43. https://doi.org/10.1159/000108587
42. Sammartino F, Krishna V, King NKK, et al. Sequence of electrode implantation and outcome of deep brain stimulation for Parkinson's disease. J Neurol Neurosurg Psychiatry 2016;87:859–863. https://doi.org/10.1136/jnnp-2015-311426
43. Pollo C, Kaelin-Lang A, Oertel MF, et al. Directional deep brain stimulation: an intraoperative double-blind pilot study. Brain 2014;137:2015–2026. https://doi.org/10.1093/brain/awu102
44. Chen CC, Pogosyan A, Zrinzo LU, et al. Intra-operative recordings of local field potentials can help localize the subthalamic nucleus in Parkinson's disease surgery. Exp Neurol 2006;198:214–221. https://doi.org/10.1016/j.expneurol.2005.11.019
45. Telkes I, Ince NF, Onaran I, et al. Localization of subthalamic nucleus borders using macroelectrode local field potential recordings. Paper presented at: 36th Annual International Conference of the IEEE Engineering in Medicine and Biology Society; 2014; Chicago, IL. https://doi.org/10.1109/EMBC.2014.6944160
46. Marmor O, Valsky D, Joshua M, et al. Local vs. volume conductance activity of field potentials in the human subthalamic nucleus. J Neurophysiol 2017;117:2140–2151. https://doi.org/10.1152/jn.00756.2016
47. Levy R, Ashby P, Hutchison WD, et al. Dependence of subthalamic nucleus oscillations on movement and dopamine in Parkinson's disease. Brain 2002;125:1196–1209. https://doi.org/10.1093/brain/awf128
48. Raz A, Eimerl D, Zaidel A, et al. Propofol decreases neuronal population spiking activity in the subthalamic nucleus of Parkinsonian patients. Anesth Analg 2010;111:1285–1289. https://doi.org/10.1213/ANE.0b013e3181f565f2
49. Tinkhauser G, Pogosyan A, Debove I, et al. Directional local field potentials: a tool to optimize deep brain stimulation. Mov Disord 2018;33:159–164. https://doi.org/10.1002/mds.27215
50. Connolly AT, Jensen AL, Bello EM, et al. Modulations in oscillatory frequency and coupling in globus pallidus with increasing parkinsonian severity. J Neurosci 2015;35:6231–6240. https://doi.org/10.1523/JNEUROSCI.4137-14.2015
51. Hammond C, Bergman H, Brown P. Pathological synchronization in Parkinson's disease: networks, models and treatments. Trends Neurosci 2007;30:357–364. https://doi.org/10.1016/j.tins.2007.05.004
52. Neumann W-J, Degen K, Schneider G-H, et al. Subthalamic synchronized oscillatory activity correlates with motor impairment in patients with Parkinson's disease. Mov Disord 2016;31:1748–1751. https://doi.org/10.1002/mds.26759
53. Steiner LA, Neumann W-J, Staub-Bartelt F, et al. Subthalamic beta dynamics mirror Parkinsonian bradykinesia months after neurostimulator implantation. Mov Disord 2017;32:1183–1190. https://doi.org/10.1002/mds.27068
54. Kühn AA, Tsui A, Aziz T, et al. Pathological synchronisation in the subthalamic nucleus of patients with Parkinson's disease relates to both bradykinesia and rigidity. Exp Neurol 2009;215:38038–7. https://doi.org/10.1016/j.expneurol.2008.11.008
55. Brown P, Oliviero A, Mazzone P, et al. Dopamine dependency of oscillations between subthalamic nucleus and pallidum in Parkinson's disease. J Neurosci 2001;21:1033–1038. https://doi.org/10.1523/JNEUROSCI.21-03-01033.2001
56. Kühn AA, Kempf F, Brücke C, et al. High-frequency stimulation of the subthalamic nucleus suppresses oscillatory β activity in patients with Parkinson's disease in parallel with improvement in motor performance. J Neurosci 2008;28:6165–73. https://doi.org/10.1523/JNEUROSCI.0282-08.2008
57. Bronte-Stewart H, Barberini C, Koop MM, et al. The STN beta-band profile in Parkinson's disease is stationary and shows prolonged attenuation after deep brain stimulation. Exp Neurol 2009;215:20–28. https://doi.org/10.1016/j.expneurol.2008.09.008
58. Rosa M, Giannicola G, Servello D, et al. Subthalamic local field beta oscillations during ongoing deep brain stimulation in Parkinson's disease in hyperacute and chronic phases. Neurosignals 2011;19:151–162. https://doi.org/10.1159/000328508
59. Ince NF, Gupte A, Wichmann T, et al. Selection of optimal programming contacts based on local field potential recordings from subthalamic nucleus in patients with Parkinson's disease. Neurosurgery 2010;67:390–397. https://doi.org/10.1227/01.NEU.0000372091.64824.63
60. Chase A. Neurosurgery: directional electrodes widen the therapeutic window for deep brain stimulation in movement disorders. Nat Rev Neurol 2014;10:364–364. https://doi.org/10.1038/nrneurol.2014.101
61. Okun MS, Rodriguez RL, Foote KD, et al. A case-based review of troubleshooting deep brain stimulator issues in movement and neuropsychiatric disorders. Parkinsonism Relat Disord 2008;14:532–538. https://doi.org/10.1016/j.parkreldis.2008.01.001

Supporting Data

Additional Supporting Information may be found in the online version of this article at the publisher's web-site.